Available online at www.sciencedirect.com
SCIENCE DIRECT®
Engineering Failure Analysis 12 (2005) 420–431
ENGINEERING FAILURE ANALYSIS
www.elsevier.com/locate/engfailanal

Analysis of failed ethylene cracking tubes

Kaishu Guan *, Hong Xu, Zhiwen Wang

Research Institute of Process Equipment, East China University of Science and Technology, 130 Meilong Rd., P.O. Box 402, 200237 Shanghai, PR China

Received 3 March 2004; accepted 30 March 2004
Available online 13 November 2004

Abstract

The failure of ethylene cracking tubes at an elevation of about 5 m in radiant chambers after one-year service has been analysed. Bulges and circumferential cracks, oriented towards the walls/burners, are the result. The investigation included tensile tests, optical microscopy, scanning electron microscopy (SEM), energy dispersive spectroscopy (EDS), and X-ray diffraction (XRD) analysis. Analysis revealed that ruptures found in the tubes were caused by overheating of the tubes because of inappropriate burning of bottom burners. Significant growth of precipitates of carbide was observed in the failed zones which results in the drastic reduction of material ductility. The bulged zones also showed a globular form of grains. Tube bowing, due to the restricted growth during the hot expansion, promotes cracks. To avoid such overheating, precautions should be taken while improving the burning condition of the bottom burners and decreasing the peak tube metal temperature. It is necessary to check the tube temperature periodically in critical positions and one should ensure that the temperature is less than the design temperature.

Keywords: Bulging failure; Cracks; Overheating; Tube failures; Chemical-plan failures

1. Introduction

Ethylene cracking tubes or reformer tubes and other tubes, which are made from cast creep resistant austenitic steel HP grade (26 Cr, 35 Ni, 0.4 C) are usually designed for a normal life of 100,000 h (11.4 years), their actual service life, however, varies from 30,000 to 180,000 h, depending on the service conditions and of course on the quality of materials [1]. Due to prolonged exposure to high temperature, the microstructure of the material is subjected to degradation. Although sufficient care is taken in the selected

* Corresponding author. Tel.: +86 21 64253055; fax: +86 21 64253810.
E-mail address: guankaishu@ecust.edu.cn (K. Guan).

1350-6307/$ - see front matter © 2004 Elsevier Ltd. All rights reserved.
doi:10.1016/j.engfailanal.2004.03.012

materials, design and operations, failures can hardly be avoided because of various reasons, such as overheating [2], stress corrosion cracking [3], creep and fatigue [4–7].

In our paper, a detailed investigation of failure in ethylene cracking tubes was presented.

2. Background

The ethylene cracking tubes are vertically installed. The feed gas, such as naphtha and steam, enters at the top end at a pressure of 0.1 MPa and flows down individual tubes. The ethylene cracking reaction takes place in the tubes and is endothermic. For this, heat is provided by burners, distributed at two sides of the furnace symmetrically. There are 36 bottom burners and 48 wall burners. The bottom burners provide about 85% of total heat intensity. The heat is transferred to the cracking tubes through radiation and the metal temperature is maintained between 700 and 900 °C by design requirement. The material specification and design parameters are given in Table 1. The composition of tubes is in agreement with the requirements of the specifications for HP40 metal.

After about one year in service, four ethylene cracking furnaces were damaged. The damage style, ruptures of a number of tubes, is almost the same. All the cracks are circumferential and at an elevation of about 5 m in the radiant chambers. Bulges also occurred at this elevation. The cracks and bulges are oriented towards the walls/burners.

In general, failure of furnace tubes can occur in a variety of modes. In this case, however, the probably reasons may be one or more of the following: (1) overheating in this zone; (2) material strength cannot meet the requirement; (3) limitation of the tube elongation. To identify the failure reason, tensile and tests, metallography and fractography analysis should be carried out by light microscope and scanning electron microscopy (SEM).

3. Experimental and results

3.1. Visual examination

Fig. 1 shows the actual bulge and rupture of as received sample. The local bulge has penetrated as shown in Fig. 1(a). Cross-sectional view of the bulge tube is shown in Fig. 1(b). Tube diameter is now increased and

Table 1
Material specification of ethylene cracking tubes of sample and design parameters

Tube material	HP40	
Composition (wt%)	C	3.8
	Si	0.65
	Mn	0.31
	P	0.07
	S	0.04
	Cr	23.4
	Ni	41.9
	Nb	1.36
	W	0.80
	Fe	Balance
Design temperature	700–900 °C	
Tube size	Outer diameter	63 mm
	Thickness	6.4 mm
	Length	12 m

elliptical. This is an extraordinary amount of deformation. It is consistent, however, with a tube that has operated at higher than normal temperatures for short periods. Fig. 2(a) shows the penetrated crack with about 2 mm open. Fig. 2(b) shows the crack viewed on the tube inner surface. The crack is discontinuous in inner surface. The penetrated crack is longer in outer surface than that in inner surface which indicates the crack originated from outer surface. There is no indication of any localized damage in the form of pits. No wall thinning and plastic deformation is observed near the crack which reveals that the crack is brittle in nature.

3.2. Tensile strength

Tensile tests at room temperature (25 °C) of the service exposed tubes were performed. The tensile test sample, which was fabricated from the longitudinal direction on slightly bulged zone, is shown in Fig. 3. The average value is taken after 3 specimens per condition were tested. The fracture surfaces through the tensile tested specimens were examined by SEM in order to identify the fracture characterizations. The values of the Ultimate Tensile Strength (UTS) and elongation % are shown in Table 2. The tests show that the tensile strength and ductility are decreased compared with standard HP40 material. The data given in Table 2 shows a rather brittle fracture.

3.3. Microstructure

In order to compare the microstructure between the bulged zone and normal OD zone, optical metallographic samples prepared from the different sites as shown in Fig. 4. 1# sample was cut from immediately near the penetrated bulge zone along the cross-section. 2# and 3# samples were cut from slightly bulged zone and normal OD zone, respectively.

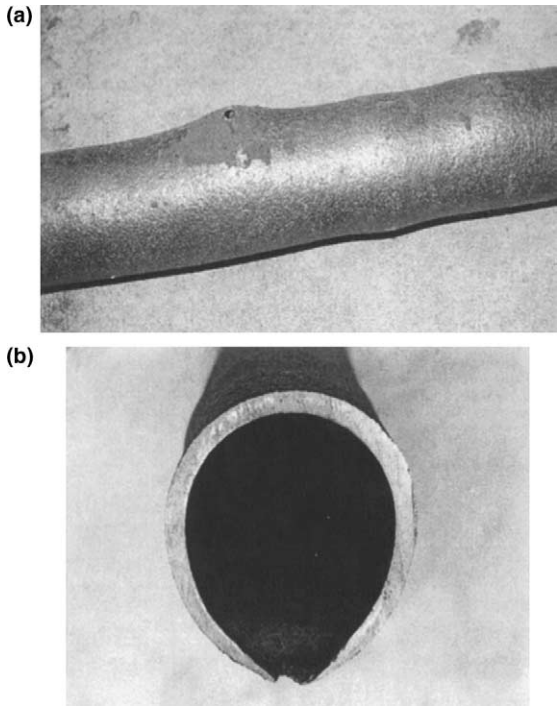

Fig. 1. Tube bulge of as received sample: (a) general view; (b) cross-section.

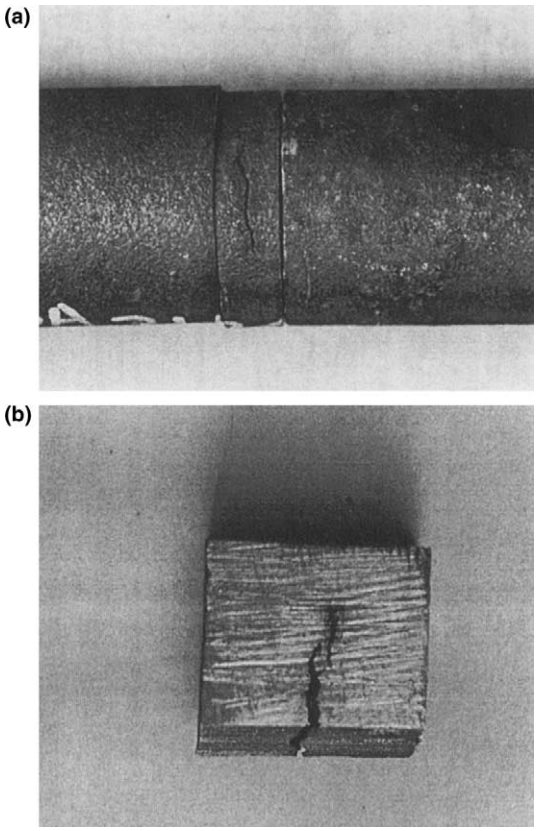

Fig. 2. circumferential crack at: (a) outer surface; (b) inner surface.

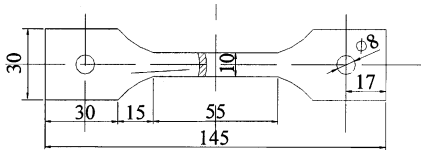

Fig. 3. Tensile test sample.

Table 2
Tensile strength of service exposed tube

	σ_b (MPa)	δ_5(%)	Ψ (%)	Temperature (°C)
Test result	317	<1	<1	25
ASTM standard	⩾430	⩾4.5		

Fig. 5(a) shows austenite matrix and a network of primary carbides of 3# sample, which is the typical microstructure of as-cast materials of alloys with high chromium and nickel contents [8,9]. But precipitates of small blocky type are found in the austenitic grains. Fig. 5(b) shows the microstructure of 2# sample. Carbides are obviously coalesced and blocky which indicates overheating. This is more pronounced in ruptured side as is shown in Fig. 5(c) of 1# sample, suggesting that it had experienced more overheating. Creep cavities and carburization are not obvious in the LOM observation.

3.4. Fractography

Fig. 6(a)–(b) shows the SEM photography of bulged penetration surface. The rupture shows intergranular fracture. The grains have a globular form with increased size due to oxidation and overheating. This can be further proved by scanning electron microscopy (SEM)/energy dispersive spectroscopy (EDS) analysis as is shown in Table 3. Because these tubes are heated externally by burners, the outer surfaces of the materials are exposed to oxidizing conditions, thus oxygen and chromium are the main composition of the grain surface. Fig. 7 shows a newly opened crack immediately near the penetrated bulge. The high-temperature oxidation is not so serious as compared with Fig. 6(a)–(b), but large amount of precipitates is present. The fractography showed, in general, brittle fracture mode. The fracture is along precipitates which is rather brittle and has secondary cracks.

Fig. 8 presents fractography of the circumferential crack. The surface has been oxidised and has creep cracks as shown in Fig. 8(a). The general view shows overloaded ductile fracture as is presented in Fig. 8(b) on another position. The detailed morphology of Fig. 7(b), shown in Fig. 8(c), however, shows the crack propagating along the precipitate. The cause can be explained as follow. Since matrix metal around these precipitates possesses good ductility and toughness, when the fracture takes place along these precipitates, the surrounding metal matrix presents ductile fracture. So the fractography looks like overloaded ductile fracture in general view.

Fig. 9 shows the micro-morphology of a tensile specimen at room temperature. The fracture surface is covered by a large amount of precipitates. These precipitates are rather brittle and give secondary cracks. The fractography showed, in general, brittle fracture mode.

3.5. Precipitates

The chemical composition of precipitates is 78.44%Cr–16.17%Fe–5.39%Ni identified by SEM/EDS. From the ratio of [Fe]/[Cr] we can deduce that the precipitates are carbides. In order to further identify the structure of precipitates, X-ray diffraction (XRD) is used to characterize the structure of the phases.

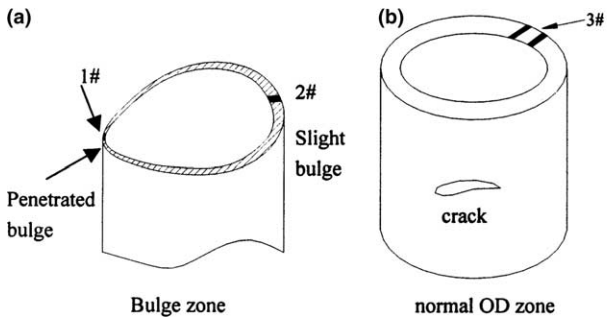

Fig. 4. Location of microstructure observation.

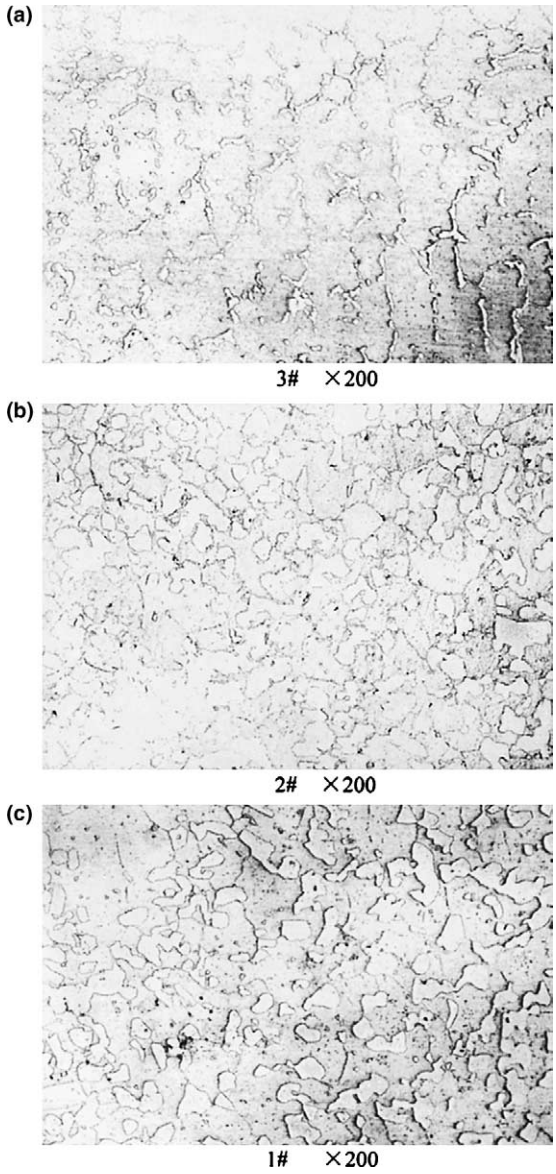

Fig. 5. Microstructure of section of failed tube.

XRD patterns obtained from the bulk metal matrix show that the precipitates are mainly $Cr_{23}C_6$ carbide (Fig. 10).

4. Discussion

From the results presented in the earlier section it appears that tubes at elevation of about 5 m failed due to long and high temperature exposure. However, the other sections of the same tube did not fail although

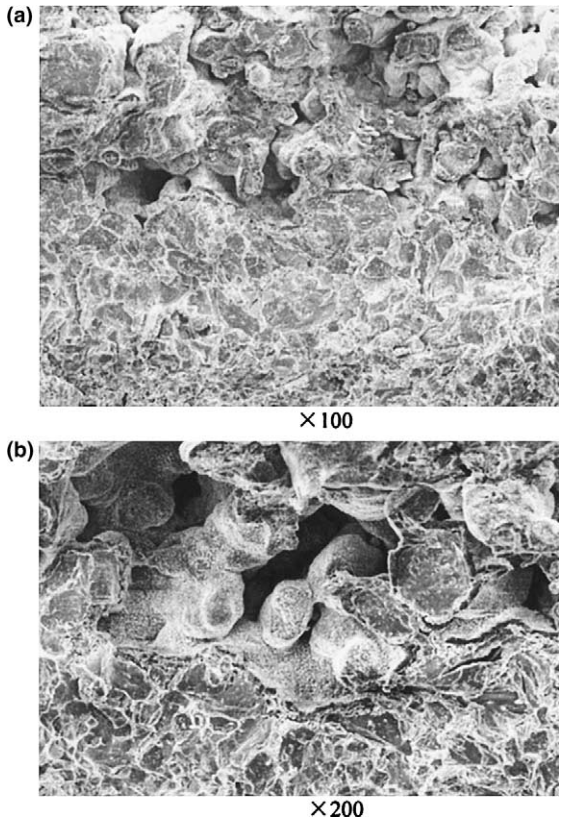

Fig. 6. Globular grains due to melting.

Table 3
Composition of globular grain by SEM/EDS

Element	wt%	at.%
OK	39.38	65.46
NaK	6.73	7.78
SK	1.47	1.22
C1K	0.85	0.64
CrK	29.56	15.12
FeK	7.07	3.37
NiK	13.81	6.25
WL	1.15	0.17

they had undergone the same period of service life. Therefore, it is understood that there was some uniqueness in the failure of tube in this section. The rise in metal temperature leads to ruptures, which can be seen from the coarsening of the carbides as well as formation of bulges. In other parts of the tubes the degree of carbides was not obvious. Generally, precipitation and growth of carbides and/or sigma phase occurs for

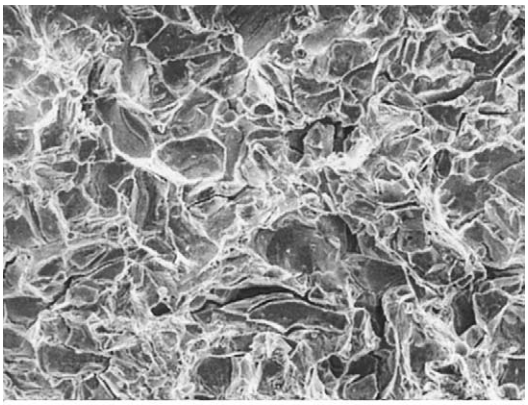

Fig. 7. SEM of newly opened crack immediately near the penetrated bulge.

this kind of material exposed to high-temperature [10–13]. However, this process needs a long time at normal service temperature. In the present case, it took only about one year. Thus, the present case of failure was due to overheating.

4.1. Reason for overheating

It is should be noticed that the tube overheating at the elevation of about 5 m is not confined to only one furnace, but occurs in four furnaces. There is a significant temperature peak resulting from bottom burners at about 5 m elevation measured by the user. Due to designed or/and fabricated factors, such as the burning and interference among the burners, the temperature in this section is higher than the design temperature. In this special case, the burner flux is already high, and the wall burners were at reduced output, so the effect is to overheat the tubes in the local position. The outer surface of the tubes at 5 m elevation is over 1200 °C measured by the user, which is higher than the tube limit of 1060 °C.

4.2. Reason for cracking

Overheating at the elevation of 5 m can cause bulges, however, the circumferential cracks in the tube are caused by not only overheating but also the tensile stress effect and reduction of ductility. The user reported that all of the failed tubes were similarly bowed when they failed. When the tube bows significantly out of plane, it is exposed excessive radiant heat as is shown in Fig. 11. The heaters are distributed at the two sides of the furnace. Generally, the tubes suffered the same temperature at two sides. However, due to tube bowing, one side is closer to the heaters than the other side. The closer side of tube will therefore operate at a higher temperature and be more likely to overheat and fail. Higher temperature will also cause the tube to grow and bend further, putting it into compression. Tube outer surface suffer from tensile stress at the bowing side as is shown in Fig. 11, thus the crack initiated from this side and from outer surface. Once the crack is formed, the crack tip is exposed directly to high-temperature oxidation. The strength of grain boundaries deteriorates and promotes intergranular cracks.

Another contributing cause to the cracking is the reduction of ductility of the material in this section because of overheating. The overheating could lead significant degradation in high temperature strength

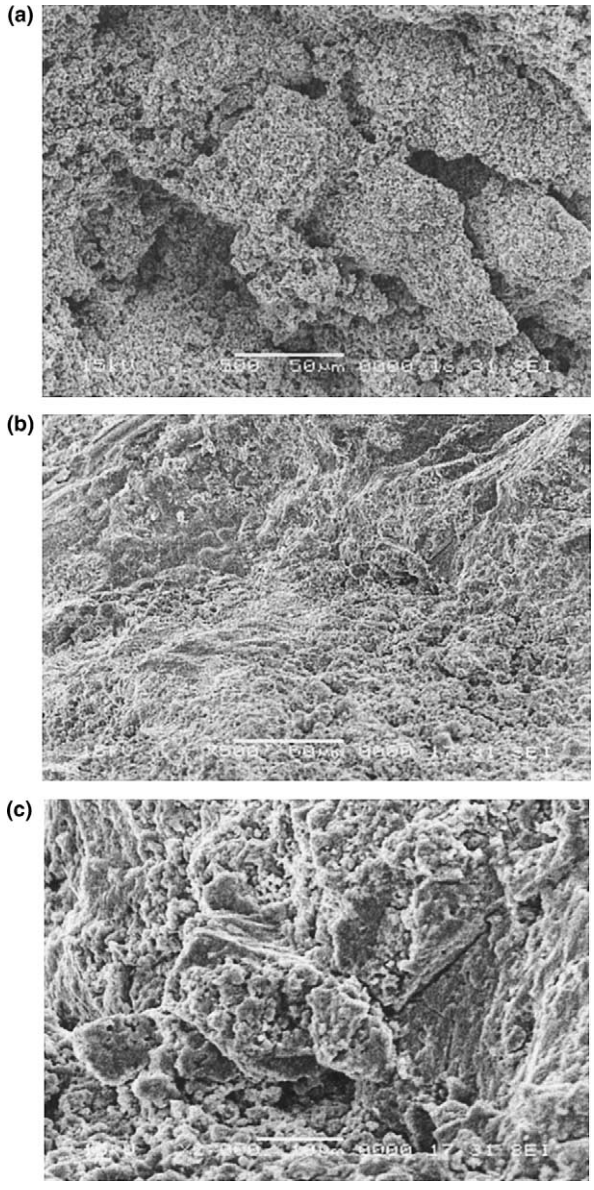

Fig. 8. SEM photography of fractured surface: (a) general view of creep cracks; (b) general view of fracture surface; (c) details of the crack surface.

and ductility during service. On the other hand, with high temperature exposure, secondary carbides precipitate in the austenitic matrix of heat resistant steels, reducing the elongation and ductility [14,15]. The ductility is of primary interest since the metal should be able to deform plastically during the tube expanding. Some steels can lose more than 80% of their original ductility while they operate at high temperature.

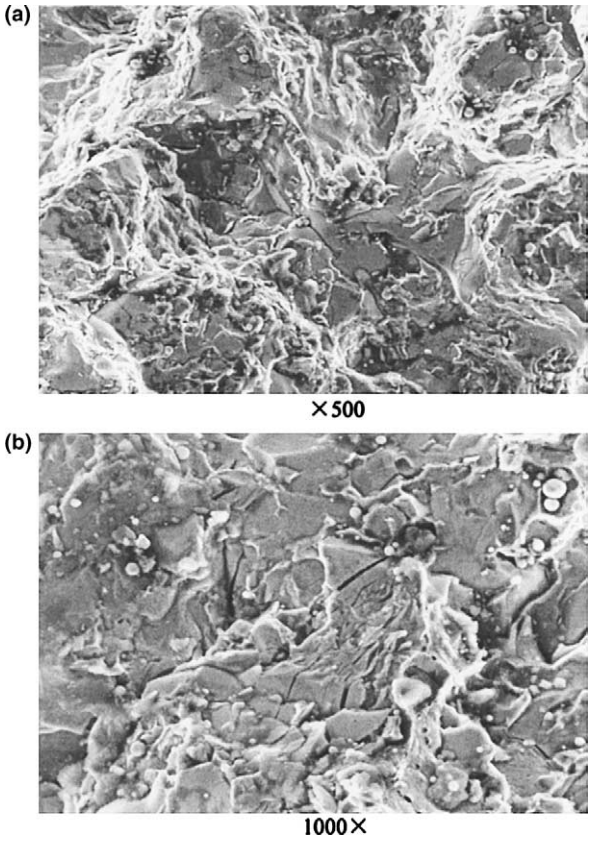

Fig. 9. SEM surface of tensile specimen.

4.3. Prevention approaches

The overheating is directly related to the bottom burners. The burners should be improved in one or two of the following ways. One is to adjust the ratio of heat intensity between the bottom burners and wall burners thus reducing the flame intensity at about 5 m height and making the temperature more uniform along the tube axis. The second way is to improve the burning conditions of the bottom burners and decrease the peak tube metal temperature.

5. Conclusions

The failure of the tubes was caused by overheating arising out of bottom burners. Significant growth of precipitates of carbide was observed in the failed zones. The bulged zones also showed a globular form of grains. Overheating during service is primarily responsible for significant degradation in mechanical properties and microstructure in the failed portion of the tubes. Tube bowing promotes the cracks. To avoid such overheating, precautions should be taken, improving the burning condition of the bottom burners and decreasing the peak tube metal temperature. It is necessary to check the tube temperature periodically in critical positions and one should ensure that the temperature is lower than the design temperature.

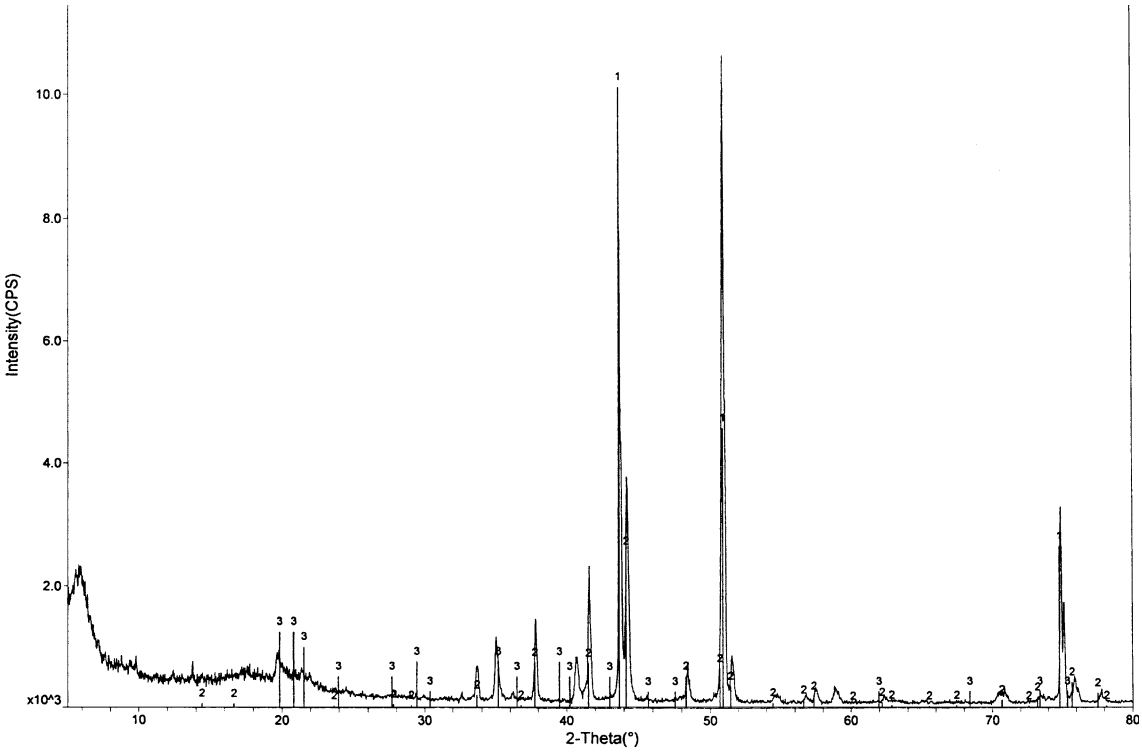

1: Austenite, 2: $Cr_{23}C_6$-Chromium Carbide, 3: could not be identified, probably is pollutant.

Fig. 10. XRD pattern of precipitate.

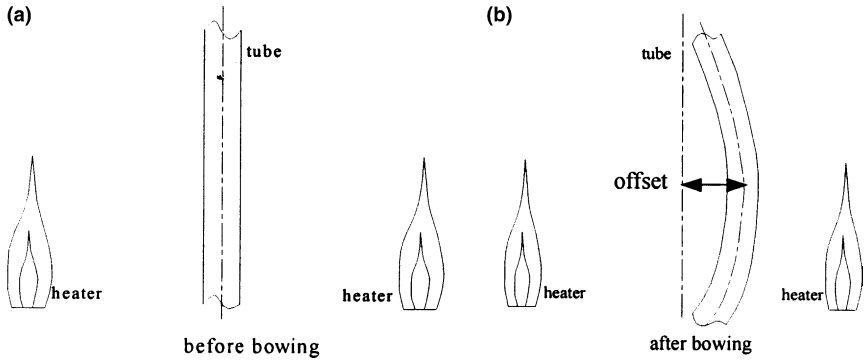

Fig. 11. Schematic drawing of tube bowing.

References

[1] May IL, Silveira TL, Vianna CH. Criteria for the evaluation of damage and remaining life in reformer furnace tubes. Int J Prv Piping 1996;66:233–41.

[2] Kumar Ray Ashok, Kumar Sinha Samarendra, Nath Tiwari Yogendra, Swaminathan Jagannathan, Das Gautam, Chaudhuri Satyabrata. Analysis of failed reformer tubes. Eng Failure Anal 2003;10:351–62.

[3] Bhaumik SK, Rangaraju R, Parameswara MA, Bhaskaran TA, Venkataswamy MA, Raghuram AC et al.. Failure of reform tube of an ammonia plant. Engi Failure Anal 2003;9:553–61.
[4] Konosu S, Koshimizu T, Lijima T, Maeda K. Evaluation of creep-fatigue damage interaction in HK 40 alloy. J Mech Des, Trans, ASME 1993;115:41–6.
[5] Shipley DG. Creep damage in reformer tubes. Int J Press Ves Piping 1983;14:21–34.
[6] Gong JM, Tu ST, Yoon KB. Damage assessment and maintenance strategy of hydrogen reformer furnace tubes. Eng Failure Anal 1999;6(3):143–53.
[7] Woo Nam Soo. Assessment of damage and life prediction of austenitic stainless steel under high temperature creep–fatigue interaction condition. Mater Sci Eng A 2002;322:64–72.
[8] Rodriguez Julian, Haro Sergio, Velasco Abraham, Colas Rafael. A metallographic study of aging in a cast heat-resisting alloy. Mater Char 2000;45:25–32.
[9] Kaya AA, Krauklis P, Young DJ. Microstructure of HK40 alloy after high temperature service in oxidizing/carburizing environment. Mater Char 2002;5486:1–11.
[10] Smith JJ, Farrar RA. Influence of microstructure and composition on mechanical properties of some AlSl 300 series weld metals. Int Mater Rev 1993;38(1):25–51.
[11] Harries DR. Physical metallurgy of Fe–Cr–Ni austenitic steels. Mechanical behaviour and nuclear applications of stainless steel at elevated temperatures. In: Proceedings of the international conference. London: The Metals Society; 1982. p. 1–15.
[12] Powell DJ, Pilkington R, Miller DA. The precipitation characteristics of 20% Cr/25% Ni–Nb stabilized stainless steel. Acta Metall 1988;36:713–24.
[13] May IL. Effects of Si content on the microstructure of modified-HP austenitic steels. Mater Char 1993;30:243–9.
[14] Haro SR, López DL, Velasco AT, Viramontes RB. Microstructural factors that determine the weldability of a high Cr-high Si HK 40 alloy. Mater Chem Phys 2000;66:90–6.
[15] Balikci Ercan, Mirshams RA, Raman A. Fracture behavior of superalloy IN738LC with various precipitate microstructures. Mater Sci Eng A 1999;265:50–62.